Manipulating the Direction of Electron Transfer in the Bacterial Reaction Center by Swapping Phe for Tyr Near $BChl_M$ (L181) and Tyr for Phe Near $BChl_L$ (M208)†

Christine Kirmaier,* Chunyan He, and Dewey Holten*

Department of Chemistry, Washington University, St. Louis, Missouri 63130

Received June 25, 2001; Revised Manuscript Received August 9, 2001

ABSTRACT: We have investigated the primary charge separation processes in *Rb. capsulatus* reaction centers (RCs) bearing the mutations Phe(L181) → Tyr, Tyr(M208) → Phe, and Leu(M212) → His. In the YFH mutant, decay of the excited primary electron donor P* occurs with an 11 ± 2 ps time constant and is trifurcated to give (1) internal conversion to the ground state (∼10% yield), (2) charge separation to the L side of the RC (∼60% yield), and (3) electron transfer to the M-side bacteriopheophytin BPh_M (∼30% yield). These results relate previous work in which the ionizable residues Lys (at L178) and Asp (at M201) have been used to facilitate charge separation to the M side of the RC, and the widely studied L181 and M208 mutants. One conclusion that comes from this work is that the Tyr (M208) → Phe and Gly(M201) → Asp mutations near the L-side bacteriochlorophyll ($BChl_L$) raise the free energy of $P^+BChl_L^-$ by comparable amounts. The results also suggest that the free energy of $P^+BChl_M^-$ is lowered more substantially by a Tyr at L181 than a Lys at L178. The results on the YFH mutant further demonstrate that the free energy differences between the L- and M-side charge-separated states play a significant role in the directionality of charge separation in the wild-type RC, and place limits on the contributing role of differential electronic matrix elements on the two sides of the RC.

The bacterial photosynthetic reaction center (RC)[1] has a macroscopic C_2 symmetry arrangement of the bacteriochlorophyll (BChl), bacteriopheophytin (BPh), and quinone (Q) cofactors (Figure 1). Excitation of the primary electron donor (P), a dimer of BChls, to its lowest excited singlet state (P*) initiates charge separation exclusively down the L side of the RC. Using $BChl_L$ in parallel mechanisms as a discrete and virtual intermediate, an electron from P* arrives on BPh_L in ∼3 ps and then moves to Q_A in ∼200 ps with an overall quantum yield of ∼1 (Figure 2A).

The Tyr residue at M208 conserved in *Rb. capsulatus*, *Rb. viridis*, and *Rps. sphaeroides* (where it is M210) was identified early-on as one of the potentially key symmetry-breaking residues in the RC (*1*−*4*). Electrostatic calculations by Parson et al. indicated that the phenolic OH dipole of this residue significantly stabilizes $BChl_L^-$ and hence is likely to contribute significantly to the mechanism, rate, and directionality of charge separation to the L branch (*5*). On the M side, the C_2 symmetry analogue of M208 is a conserved Phe at L181. The effects of Tyr M208 on L-side electron transfer have been explored experimentally in a wide variety of RCs that have mutations at M208 and L181 (*6*−*17*). Significantly longer P* lifetimes, ranging from ∼10 ps to as much as ∼40 ps at room temperature, are found in mutants with Tyr M208 changed to Phe, Thr, Ile, or Trp (compared to 3−4 ps in wild-type RCs).

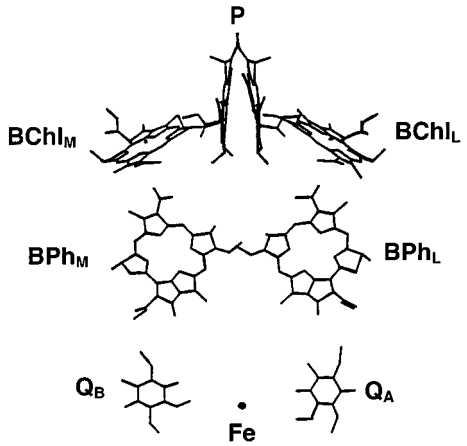

FIGURE 1: Arrangement of the RC cofactors as determined by X-ray structures of RCs from *Rb. viridis* and *Rb. sphaeroides* (*1*−*4*).

M208 and L181 are both sufficiently close to P to have an effect on its oxidation potential, a point first made by Chan et al. (*8*). In the Y(M208)F mutant, for example, the oxidation potential of P is 513 meV in *Rb. capsulatus* and 530 meV in *Rb. sphaeroides*, compared to ∼500 meV in both wild-type RCs. Recent molecular-dynamics simulations by Alden et al. indicate that replacing Tyr M210 in *Rb. sphaeroides* with Phe, Ile, or Trp increases the free energy of $P^+BChl_L^-$ by ∼200 meV, of which 40−70 meV is due to an increase in the P/P^+ potential (*18*). Similarly, electrostatic calculations by Gunner et al. indicate that Tyr M208 has a substantially larger effect on the redox properties of $BChl_L$ than P (*19*).

† This work was supported by Grant MCB0077187 from the National Science Foundation.

* Address correspondence to either of these authors at the Department of Chemistry, Washington University, St. Louis, MO 63130. Tel: 314-935-6480(6502). Fax: 314-935-4481. E-mail: kirmaier@wuchem.wustl.edu, holten@wuchem.wustl.edu.

[1] Abbreviations: RC, reaction center; BChl, bacteriochlorophyll; BPh, bacteriopheophytin; P, dimeric BChl primary electron donor; Q, quinone; L and M, polypeptide subunits of the RC.

10.1021/bi0113263 CCC: $20.00
Published on Web 09/11/2001

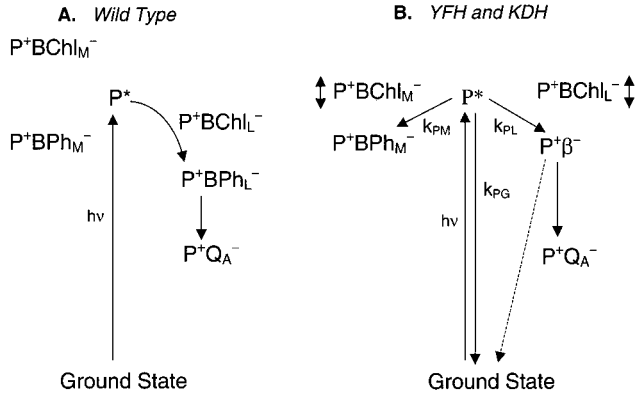

FIGURE 2: Schematic energy level diagrams for (A) wild type and (B) the YFH and KDH mutants. In the mutants, $P^+BChl_L^-$ is higher and $P^+BChl_M^-$ lower in free energy than in wild type, and the double-headed arrows reflect uncertainty as to whether these states are slightly above or slightly below P*. The rate constants k_{PL}, k_{PM}, and k_{GS} are used in a simplified kinetic analysis discussed in the text.

A working model for the RC in which $P^+BChl_L^-$ is below P* by 50−100 meV and $P^+BChl_M^-$ is above P*, but probably by no more than ∼250 meV, is largely accepted (Figure 2A) (*5*, *18*−*28*). It also seems clear that Tyr M208 and Phe L181 play significant roles in the relative free energies of these states. In the M208 mutants for which calculations place $P^+BChl_L^-$ above P*, the P* lifetimes are longer than in wild-type RCs and increase at low temperature (*7*, *10*, *11*, *18*). This is in contrast to wild-type RCs where the P* lifetime decreases at low temperature (*29*, *30*).

M208 is not the only residue that has a demonstrated effect on the free energy of $P^+BChl_L^-$. We have reported an ∼15% yield of electron transfer to BPh_M in the *Rb. capsulatus* DH mutant, G(M201)D/L(M212)H (*31*). We have suggested this results from a 100−150 meV destabilization of $P^+BChl_L^-$ by the presence of the Asp at M201 near $BChl_L$. This would put $P^+BChl_L^-$ very close to and likely slightly above P*. This strategy was taken one step further in the KDH mutant, S(L178)K/G(M201)D/L(M212)H, which has an ∼23% yield of $P^+BPh_M^-$ formation (*23*). We ascribed this increase to the added effect of lowering the free energy of $P^+BChl_M^-$ by Lys L178 near $BChl_M$.[2]

In this work, we set out to probe electron transfer to the M side in the triple mutant F(L181)Y/Y(M208)F/L(M212)H, denoted YFH. This mutant was judiciously chosen for the following reasons. First, Jia et al. have shown that changing F toY at L181 and Y to F at M208 in *Rb. capsulatus* negate each other's effects on the oxidation potential of P (*10*), as was subsequently found in calculations (*18*). Jia et al. reported 497 ± 5 and 502 ± 5 meV for the P/P^+ potential in YF and wild-type RCs, respectively [where YF denotes the F(L181)Y/Y(M208)F mutant] (*10*). This result, when combined with the expected effects on the $BChl^-/BChl$ potentials, indicates that in swapping the F/Y residues at L181/M208, the only charge-separated states whose free energies will be significantly affected are $P^+BChl_L^-$ and $P^+BChl_M^-$—the former raised and, by analogy, the latter lowered.[3] In the most simple analysis, in mutants having the L181/M208 swap of F/Y to Y/F, one would expect to find a slower rate of electron transfer to the L side and simultaneously a faster rate of electron transfer to the M side.

A second design element of YFH is the use of the L(M212)H mutation, which results in incorporation of a BChl (denoted β) in place of BPh_L (*31*, *33*−*35*). The "H" (or "beta") mutation affords the ability to probe cleanly for electron transfer to the M side via bleaching of the ∼530 nm Q_X band of BPh_M, since the partially overlapping transient bleaching due to electron transfer down the L branch is moved from ∼545 nm (BPh_L) to ∼600 nm ($\beta/BChl_L$). Previous work on L181 and M208 mutations was carried out on RCs having the native pigment content of four BChls and two BPhs. This necessarily makes probing for electron transfer to BPh_M very challenging, and electron transfer to the M side has not been reported in any of the time-resolved absorption studies done to date on L181/M208 RCs. In principle, in the mutants where the P* lifetime is very long, 20 ps or more, electron transfer to $P^+BPh_M^-$ might be expected to occur to the extent of a few percent at least. But again, such low yields would be difficult to detect in the dominating presence of $P^+BPh_L^-$ formed by parallel electron transfer down the L side. Also, the M208 single mutants that increase the oxidation potential of P are disadvantaged in terms of M-side electron transfer because $P^+BChl_M^-$ will be moved further above P*. Here again we return to the strategy of simultaneously swapping F to Y at L181 and Y to F at M208 so that the oxidation potential of P is unchanged.

With these considerations in mind, we expected that the overall primary photochemistry of the YFH and KDH mutants might be very similar. This has been borne out by the present work. We report here that in fact the YFH mutant is even more successful in supporting electron transfer to the M side, giving an ∼30% yield of $P^+BPh_M^-$ formation. These results give insights into the effects of polar or ionizable residues near $BChl_L$ and $BChl_M$ on the free energies of $P^+BChl_L^-$ and $P^+BChl_M^-$, and allow us to further address the origins of directionality in the native RC.

EXPERIMENTAL PROCEDURES

A phenylalanine was introduced at M208 using the "QuikChange" site-directed mutagenesis kit from Strategene with the M-gene DNA containing our previously constructed L(M212)H mutation serving as the template. The mutagenic primers changed the TAC codon for Tyr at M208 to TTC for Phe and also changed the bases coding for Ser M210 (TCG to AGC). This silent mutation resulted in creation of a *Bss*HII restriction-enzyme site that was used for screening of candidate mutants. Similarly, a tyrosine was introduced into the wild-type L-gene template at L181, changing the TTC codon for Phe to TAC for Tyr. Again, we also introduced a silent mutation that yielded a *Bst*XI site used for screening purposes at Leu L175 (CTG to CTT). Successful mutagenesis was verified by DNA sequencing utilizing Perkin-Elmer's "Big-Dye" kit. The mutagenized L-

[2] M201 and L178 are sufficiently far from P that one does not expect mutations at these sites to significantly affect the P/P^+ potential. This point had been confirmed by redox titrations of P in the G(M201)D *Rb. capsulatus* mutant (*31*) and the G(M203)D *Rb. sphaeroides* mutant (*32*).

[3] The changes of F to Y at L181 and Y to F at M208 are expected to have minimal effects (≤15 meV) on the BPh_M^-/BPh_M and the BPh_L^-/BPh_L potentials, respectively, based on calculations and experiments on *Rb. sphaeroides* M210 mutants (*7*, *18*).

and M-gene fragments were then both cloned into polyHis-pU2924. PolyHis-pU2924 is a derivative of the expression vector pU2924 originally devised by Bylina and Youvan (*36*) that contains seven sequential His residues added immediately before the stop codon at the end of the M gene. The polyHis-pU2924 vector was constructed and generously provided to us by Drs. D. K. Hanson and P. D. Laible (*37*).

RCs were isolated via a procedure modified slightly from the standard ammonium sulfate precipitation and DEAE chromatography methods to take advantage of the presence of the poly-His tag on the protein (*37*, *63*). Following LDAO solubilization of the RCs, Qiagen Ni-NTA resin was added to the raw LDAO/RC/chromatophore solution and the mixture slowly agitated on ice for 90 min. The slurry was then poured into a column to collect the RC-bound resin. The resin was washed with buffer 1 (10 mM Tris, pH 7.8/0.05% LDAO) until the eluent had $A < 0.05$ between 280 and 900 nm. The RCs were eluted with buffer containing 40 mM imidazole and dialyzed overnight in buffer 1. The YFH mutant gave yields of RCs similar to wild-type, ~50 ODVs (at 800 nm) per liter of cells. The occupancy of the secondary quinone (Q_B) was found to be <2% in the YFH samples. This was determined by monitoring P^+Q^- charge-recombination on the millisecond−seconds time scale, using excitation with a saturating 3 ns, 532 nm flash and probing the P-bleaching recovery kinetics at 850 nm. It was found that >98% of the decay occurred with a time constant of ~200 ms, which can be ascribed to $P^+Q_A^-$ charge recombination.

The time-resolved absorption spectrometer is based on an Ar^+-pumped regeneratively amplified Ti:sapphire OPA system operated at 10 Hz. The RCs were excited with ~130 fs pulses at 850 or 760 nm and probed with ~130 fs "white-light" flashes. The excitation pulses were defocused and/or attenuated such that ~30% of the RCs were excited on a single flash. Further details of the apparatus, data acquisition, and data analysis methods have been described elsewhere (*38*, *39*). All studies were carried out on flowed samples at ~285 K.

As a baseline for comparisons to the his-tagged YFH protein, we have carried out extensive subpicosecond time-resolved absorption experiments on a number of his-tagged RC proteins (wild-type and mutants) during the course of the last 2 years (ref *63* and unpublished results). In no case have we found a significant difference in any of the spectral or kinetic data from those reported previously on the non-polyHis analogue. However, since we wish to make quantitative comparisons of the yields of M-side electron transfer, we have repeated here (and quantitatively reproduced) our previous $P^+BPh_M^-$ yield measurements in the Q_X and anion regions on his-tagged H ≡ L(M212)H and DH ≡ G(M201)D/L(M212)H RCs, along with similar measurements on his-tagged wild-type RCs.

RESULTS

The ground-state spectrum of YFH RCs is shown in Figure 3 and is essentially identical to that of the H single mutant, L(M212)H. Excitation of YFH RCs with a near-infrared flash initially produces the excited primary donor P*. The transient absorption difference spectrum of P* is dominated by bleaching of the 850 nm ground-state absorption band of P

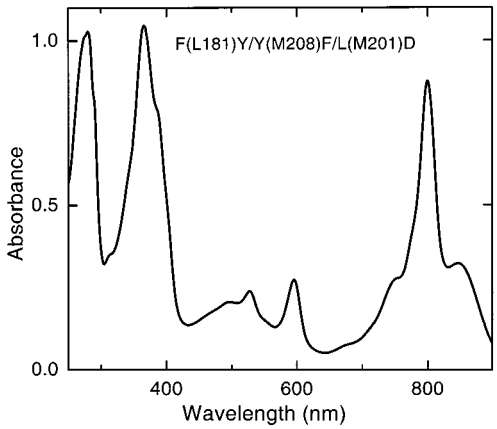

FIGURE 3: Room-temperature ground-state absorption spectrum of His-tagged RCs from the YFH mutant.

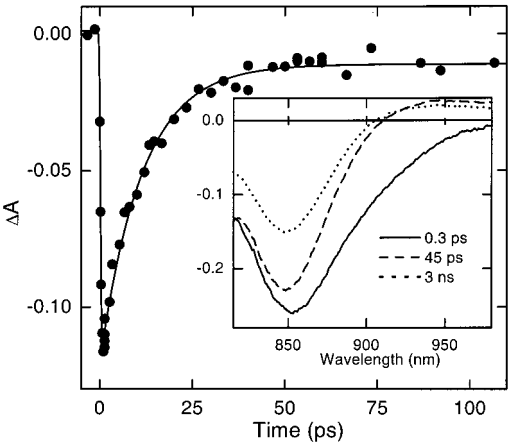

FIGURE 4: Stimulated emission decay for the YFH mutant between 900 and 910 nm (circles) and a fit to the instrument function plus a single-exponential plus a constant. The inset shows transient absorption difference spectra acquired using a 130 fs, 750 nm excitation flash in the P bleaching region.

and concomitant stimulated emission (~850−950 nm) from P* (0.3 ps spectrum in Figure 4, inset). Fits of the stimulated emission decay data between 890 and 920 nm to a single-exponential plus a constant give a P* lifetime of 11 ± 2 ps (Figure 4). In wild-type RCs, the magnitude of P bleaching remains constant as P* decays and to many nanoseconds after excitation, signaling the formation of $P^+Q_A^-$ from P* with essentially unity yield. However, in the YFH mutant the amplitude of P bleaching following P* decay (45 ps spectrum) is reduced by ~10%, and at 3 ns is reduced to ~60% of its initial magnitude (Figure 4, inset). As we shall describe below, the latter value reflects the yield of $P^+Q_A^-$.

P-bleaching decay, which directly reflects return of RCs to the ground state, is best monitored at 830−840 nm (on the blue side of the P absorption band), where the contribution of P*-stimulated emission to the absorption difference spectrum is minimal or absent. The P-bleaching decay in this region can be fit to two exponentials plus a constant (data not shown). The two time constants are 14 ± 5 ps and ~1 ns. The shorter component has an amplitude of 10 ± 3% of the initial magnitude of P bleaching, and a time constant (14 ps) that is in good agreement with the P* lifetime obtained from decay of stimulated emission. These data thus indicate that P* decay is accompanied by ~10% return to the ground state. The slower component, corre-

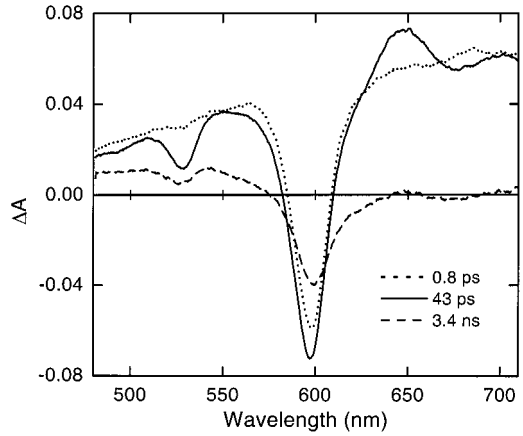

FIGURE 5: Transient absorption difference spectra taken in the Q_X and anion region acquired at the time shown following excitation with 130 fs flashes at 850 nm.

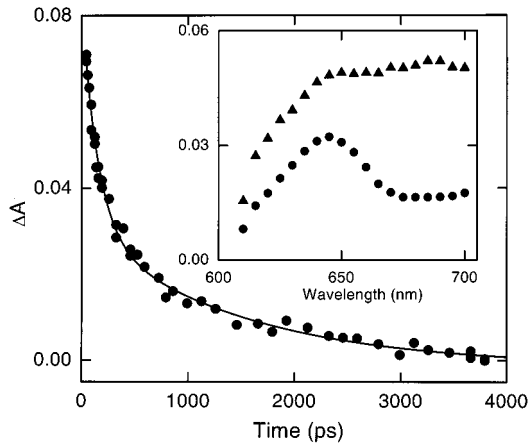

FIGURE 6: Kinetic data for the transient absorption changes between 640 and 650 nm acquired using 130 fs flashes at 850 nm (circles). The solid line is a fit to the sum of two exponentials plus a constant. Data acquired before and during the flash and during the P* lifetime have been omitted as described in the text. The inset shows the values of the preexponential factors of the dual exponentials fits across the entire anion absorption region. The triangles correspond to the ~160 ps component, and the circles correspond to the 1−4 ns component.

sponding to the ~30% further recovery of P bleaching between 45 ps and 3 ns in Figure 4 (inset), is assigned to charge recombination (to the ground state) of the M-side state $P^+BPh_M^-$.[4] The initial formation of $P^+BPh_M^-$ from P* is based on spectral data in the Q_X and anion regions, to which we now turn.

Absorption difference spectra spanning 480−710 nm are shown in Figure 5. The spectrum taken 0.8 ps after excitation, with its featureless absorption broken by bleaching of the Q_X band of P at ~600 nm, is characteristic of P*. The spectrum at 43 ps has a pronounced bleaching at ~527 nm, which we assign to bleaching of the ground-state Q_X absorption band of BPh_M. This spectrum also has a distinct absorption band at ~645 nm that is characteristic of the BPh_M anion in state $P^+BPh_M^-$. Both of these assignments are the same as in the DH, KDH, and related mutants (*23*, *24*, *31*). The time-evolution of the absorbance changes across the anion region (620−700 nm) was analyzed using data from ~40 ps to ~3.8 ns. This follows the procedure that we have used previously, where time points before and during the excitation flash and during the P* lifetime were removed from the kinetic data set in order to reduce the number of parameters in the fits. As is seen in Figure 6, the time evolution of ΔA between 640 and 650 nm in the YFH mutant clearly is not single-exponential and requires a fit to the sum of two exponentials plus a constant (solid line). The same is true of the data throughout the entire region between 620 and 700 nm, with average fitted time constants of 160 ± 30 ps and 1.0 ± 0.3 ns. Because the data extend to only 3.8 ns and this at best is about four 1/e times of the slower component, the error in the associated time constant is much larger than indicated by a simple best fit. [This discussion also applies to the ~1 ns component of the P-bleaching decay.] Holding the slow component fixed at 1.5, 2.0, 2.5, or 3.0 ns also give good fits with the value of the faster time constant only marginally changed. The use of time constants longer than about 4 ns for the slow component gives poorer fits and unreasonable spectra at the asymptote of the decay. These considerations suggest that the time constant of the slower component is in the 1−4 ns range. Essentially the same results and conclusions were obtained previously for the DH and KDH mutants.

The inset to Figure 6 gives a plot of the preexponential values from the dual-exponential fits to the anion-region data. These amplitude spectra were generated from fits in which the value of the longer component was held fixed at 2 ns. (Varying this time constant between 1 and 3 ns does not appreciably affect the spectra that result.) The spectrum of the 160 ps component (triangles) shows a broad absorption covering the entire region with two apparent maxima at ~640 and ~690 nm. In keeping with the analysis given previously for KDH RCs (*23*), the faster anion-region decay component in the YFH mutant is assigned to decay of the L-side charge-separated intermediate, generically denoted P^+I^-. As is indicated in Figure 2B, in YFH (and DH and KDH) RCs we expect that this L-side transient is largely $P^+\beta^-$, with perhaps some mixing with $P^+BChl_L^-$ depending on how close these two states are in (free) energy.[5] The ~160 ps kinetic component reflects $P^+I^- \rightarrow P^+Q_A^-$ electron transfer (with perhaps a few percent concomitant $P^+I^- \rightarrow$ ground state). The preexponential factor spectrum of the longer-lived component (circles in Figure 6 inset) has a distinct maximum at ~645 nm. As discussed above, this absorption is consistent with the BPh_M anion. Thus, we assign the 1−4 ns kinetic component observed in the anion region and in the P bleaching data to the decay of $P^+BPh_M^-$ via charge recombination to the ground state. (Recall that Q_B is absent.)

Figure 7 compares the magnitudes of Q_X BPh bleaching in RCs from wild-type and the H, DH, and YFH mutants acquired using 850 nm excitation. For each RC, the spectrum shown was taken at a delay time that corresponds to about

[4] We cannot rule out the presence of a third, small-amplitude component (several percent) in the P bleaching decay kinetics that might reflect some charge-recombination of the L-side intermediate to the ground-state competing with $P^+Q_A^-$ formation.

[5] The nature of the L-side intermediate P^+I^- differs depending on the (free) energy gaps between the L-side states and thus the quantum/thermal mixing between them. From this and previous work, it can be concluded that P^+I^- is $P^+BPh_L^-$ in the wild-type RC, is largely $P^+\beta^-$ (perhaps with minor contribution from $P^+BChl_L^-$) in the YFH and DH and KDH RCs, and is a substantial mixture of $P^+\beta^-$ and $P^+BChl_L^-$ in the H mutant (*23*, *24*, *31*, *33*−*35*).

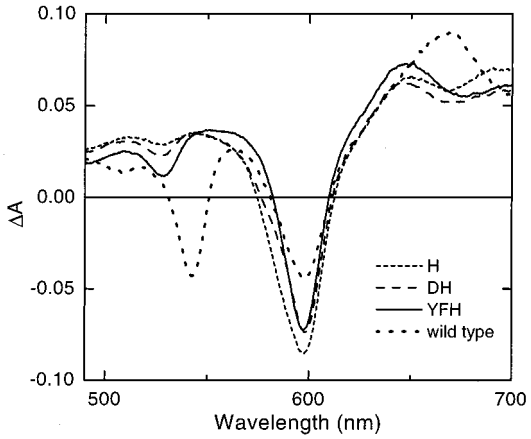

FIGURE 7: Comparison of the Q_X and anion region transient absorption spectra in H, DH, YFH, and wild-type RCs acquired using 130 fs flashes at 850 nm, normalized to the same initial P* concentration. The spectra were acquired at about four P* lifetimes for each RC, namely, at 35, 60, 45, and 15 ps, respectively.

Table 1: P* Lifetimes, Decay Products, and Associated Rate Constants[a]

RC	P* lifetime (ps)	% yield ground state	% yield P^+I^-[b]	% yield $P^+BPh_M^-$	k_{PG} (ps^{-1})	k_{PL} (ps^{-1})	k_{PM} (ps^{-1})
wt	4.3 ± 0.3	nd[c]	100	nd	–	4.2	–
H	8.5 ± 0.8	nd	93	7	–	8.6	114
DH	15 ± 2	15	70	15	100	21	100
KDH	15 ± 2	15	62	23	100	24	65
YFH	11 ± 2	10	60	30	110	18	37

[a] All data were taken at ~285 K. The measured yields of the states have an error of ~5%. The results for wild-type, H, and DH found here reproduce those reported in (*23, 31*). The data for the KDH mutant are taken from ref *23*. [b] P^+I^- denotes the L-side intermediate, which is $P^+BPh_L^-$ in wild-type RCs. P^+I^- is a quantum/thermal admixture of $P^+BChl_L^-$ and $P^+\beta^-$ in the other mutants, more heavily weighted to the latter in DH, KDH, and YFH RCs.[5] [c] Not detected.

four P* lifetimes and thus reflects the maximal Q_X bleaching observed. The spectra have been normalized slightly, by factors that ranged between 1 and 1.2, to account for slight differences in concentration and/or laser conditions. In each case, the factor applied was determined by normalizing the 0.3 ps P* spectra so that the initial magnitude of bleaching of the ~600 nm Q_X (and 850 nm Q_Y) band of P was identical in all four samples (data not shown). Comparing the integrated magnitudes of the 527 nm bleaching in the H, DH, and YFH mutants with that of the 542 nm BPh_L bleaching in wild-type RCs, we calculate that the yields of $P^+BPh_M^-$ formation are 7%, 15%, and 30%, respectively, in the three mutants compared to the 100% yield of $P^+BPh_L^-$ in wild-type RCs. The underlying assumption is that the Q_X bands of BPh_L and BPh_M have the same oscillator strength (*23*, *31*). The yields obtained here for his-tagged H and DH compared to his-tagged wild-type are identical to the yields obtained previously for the non-His-tagged versions of these mutants compared to non-His-tagged wild-type. These results, along with those for the KDH mutant (not repeated here), are collected in Table 1.

DISCUSSION

Swapping the native Phe L181 and Tyr M208 residues near $BChl_M$ and $BChl_L$, respectively, in conjunction with the "beta" mutation at M212, clearly has resulted in a significant yield of electron transfer to the M-side BPh in the YFH mutant. This result links together numerous studies on the L181 and M208 mutants and the DH and KDH mutants where we introduced ionizable residues at L178 (near $BChl_M$) and M201 (near $BChl_L$). Based on previous work, one would have predicted that the YFH and KDH mutants would have a similar propensity for electron transfer to the M side of the RC, and this has been demonstrated here. A commonality between these mutants is found in a simple raising of the free energy of $P^+BChl_L^-$, thus slowing electron transfer to the L side, and a simultaneous lowering of the free energy of $P^+BChl_M^-$, thus increasing the rate of electron transfer to the M side. In the one case (KDH) this has been done by addition of ionizable Asp and Lys residues and in the other (YFH) by adding/removing polar Tyr residues. Of course there are differences in detail to which we now turn in a closer examination of the relative free energies of $P^+BChl_L^-$, $P^+BChl_M^-$, and P*, and the relative rates and contributions to directionality of electron transfer to the L and M sides.

Starting with the DH mutant, we adopt a simple branching scheme shown in Figure 2B, with effective rate constants k_{PM}, k_{PL}, and k_{PG} for P* → $P^+BPh_M^-$, P* → P^+I^-, and P* → ground state (where P^+I^- is the L-side charge-separated intermediate[5]). The ~15 ps P* lifetime and yields of $P^+BPh_M^-$ (15%), $P^+BPh_L^-$ (70%), and internal conversion to the ground state (15%) yield the rate constants shown in the last three columns of Table 1. Let us suppose that placing an Asp at M201 and removing Tyr at M208 have about the same effect on the free energy of $P^+BChl_L^-$ and ask what one would predict for the YFH mutant. Given the assumption, k_{PL} would be the same in the YFH and DH mutants. Holding $k_{PL} = (21ps)^{-1}$ and $k_{PG} = (100\ ps)^{-1}$ (both from the DH mutant), one can ask what the predicted P* lifetime would be in the YFH mutant, where a 30% yield of $P^+BPh_M^-$ is obtained. The answer is 12 ps (or 13 ps using the values from the KDH mutant), which is the same within error as the P* lifetime we have measured here for the YFH mutant.

One can also approach this argument using the YFH data alone. Using the measured 11 ps P* lifetime and yields of return to the ground state (10%) and charge separation to the L side (30%) and M side (60%), the rate constants given in Table 1 are calculated. The calculated k_{PG} of $(110\ ps)^{-1}$ for the YFH mutant is in very good agreement with the $(100\ ps)^{-1}$ rate constant obtained previously for the DH and KDH mutants, consistent with the expectation that P* internal conversion should not be radically different in these mutants. In the YFH mutant, k_{PL} is calculated to be $(18\ ps)^{-1}$, compared to $(21\ ps)^{-1}$ and $(24\ ps)^{-1}$ in the DH and KDH mutants, respectively. Given the similar rates of charge separation to the L side, we infer that the free energy of $P^+BChl_L^-$ is comparable in the YFH, DH, and KDH mutants.

Alden et al. have calculated that changing Tyr at M208 to Phe destabilizes $P^+BChl_L^-$ as much as ~200 meV (depending on orientation of the Tyr M208 OH dipole), of which some 40 meV is due to an increase in P's oxidation potential (*18*). Based on these calculations, $P^+BChl_L^-$ could be destabilized by up to ~160 meV in the YFH mutant, where the effect on the oxidation potential of P is negated by the L181/M208 swap of F/Y to Y/F. Gunner et al. also have calculated a significant (but perhaps somewhat smaller) effect on the $BChl_L$ potential (*19*). Our experimental results

suggest that an Asp at M201 raises the free energy of $P^+BChl_L^-$ by 100−150 meV (*23*, *31*). Collectively, these free energy estimates are consistent with our conclusion, based on finding similar rate constants for L-side charge separation, that the free energy destabilization of $P^+BChl_L^-$ is comparable in the YFH, KDH, and DH mutants.[6] Assuming that $P^+BChl_L^-$ is 50−100 meV below P* in the wild-type RC (*5*, *18*−*24*, *28*), these considerations support a working model in which $P^+BChl_L^-$ is near and probably slightly above P* in these mutants. A slowing of the rate constant for L-side charge separation [e.g., $\sim(20\ ps)^{-1}$ in the YFH mutant compared to $\sim(8\ ps)^{-1}$ in the H mutant] would follow, regardless of the relative contributions of the parallel two-step chemical intermediate ($P^* \rightarrow P^+BChl_L^- \rightarrow P^+BPh_L^-$) and one-step superexchange ($P^* \rightarrow P^+BPh_L^-$) roles of $BChl_L$. Similar arguments, along with the temperature dependence of the P* lifetime, have been offered previously in discussing that $P^+BChl_L^-$ may be isoenergetic or above P* in a number of the M208 single mutants and the DH and KDH RCs (*6*−*13*, *23*, *24*, *31*).

Much less is known about the free energies of the M-side charge-separated states, but it is thought that both $P^+BChl_M^-$ and $P^+BPh_M^-$ are at higher free energy than their L-side counterparts (*5*, *18*, *19*, *41*−*43*). Calculations place $P^+BPh_M^-$ at least 130 meV above $P^+BPh_L^-$ (*18*, *19*), the latter being below P* by ∼250 meV when relaxed (*21*, *25*−*28*). The hydrogen bond between Glu L104 and the ring-V keto group of BPh_L and the absence of an analogous hydrogen bond to BPh_M almost certainly contribute significantly to the relative stabilization of $P^+BPh_L^-$. Calculations place $P^+BChl_M^-$ above $P^+BChl_L^-$ by 150−350 meV (*5*, *18*, *19*, *41*−*43*), or above P* by <250 meV (*18*). Katilius et al. recently reported a key experimental result that helps bracket the free energy gap between $P^+BPh_M^-$ and $P^+BChl_M^-$ (*44*). By removing the His ligand to $BChl_M$ in the *Rb. sphaeroides* H(M182)L mutant, they have replaced $BChl_M$ with a BPh, denoted ϕ_M. Charge separation occurs in this mutant to give $P^+\phi_M^-$ in ∼35% yield with no apparent further electron transfer onto BPh_M, indicating that $P^+\phi_M^-$ is lower in free energy than $P^+BPh_M^-$. Other things being equal, this result indicates that the free energy gap between $P^+BPh_M^-$ and $P^+BChl_M^-$ can be no larger than the difference in the reduction potentials of BChl and BPh. In solution, this difference ranges between 180 and 300 mV (*45*−*48*); values near the lower end of this range are indicated in situ upon replacing BPh_L with a BChl (β) in the L(M212)H mutants (*24*). These considerations yield a working model that has $P^+BChl_M^-$ above P* and $P^+BPh_M^-$ below P* with a free energy gap between the two charge-separated states no larger than ∼250 meV.

What are the implications for the YFH mutant? Our finding that $P^+BPh_M^-$ forms and lives 1−4 ns shows that $P^+BPh_M^-$ is below P* and that $P^+BChl_M^-$ is not below $P^+BPh_M^-$ in this mutant (or DH or KDH). Thus, the YFH mutant has not reached the extreme set by the H(M182)L mutant (*44*). Calculations indicate that a Tyr at L181 would significantly stabilize $P^+BChl_M^-$, though perhaps not quite as much as Tyr M208 stabilizes $P^+BChl_L^-$ (*18*). Thus, the maximum stabilization of $P^+BChl_M^-$ in the YFH mutant should be ∼150 meV (give or take 50 meV), which is a large portion of the total available gap between $P^+BChl_M^-$ and $P^+BPh_M^-$. Concerning a lower limit to the amount that $P^+BChl_M^-$ has been stabilized, our results indicate that it is not zero, and is greater than that afforded by placing a Lys at L178 in the KDH mutant.

Regardless of whether $P^+BChl_M^-$ is above or below P* in the YFH mutant, some interesting discussion follows regarding the contributions of energetics and electronic matrix elements to the directionality of charge separation to the L versus M sides of the RC. Let us first consider the case where Tyr L181 has lowered the free energy of $P^+BChl_M^-$ sufficiently that it is below P* in the YFH mutant. This will make the M side of the YFH RC essentially identical to the L side of one of the first RC mutants made, namely, the *Rb. capsulatus* Glu (L104) → Leu mutant. In both cases, P* is highest in free energy, followed at lower free energy by the P^+BChl^- charge-separated state and below that a P^+BPh^- state that is at somewhat higher free energy than in wild-type. The higher placement of P^+BPh^- owes, again, in both cases to the absence of the hydrogen bond to the ring-V keto group of the BPh macrocycle. Thus, we have a direct comparison of L and M chromophore chains as identical in both composition and the free energies of the states as one might hope to achieve through *minimal* manipulation of the RC, even including in both cases the Tyr between P and BChl. Regardless of whether the true mechanism of electron transfer is one step or two steps or a combination, since the two chains are "matched" we can assume the mechanism will be the same.[7] Thus, we can make a direct comparison of the effective rate constants, and from there the effective electronic matrix elements, for charge separation to the L and M sides of the RC. In the YFH mutant, we have measured here an M-side rate constant $k_{PM} \sim (37\ ps)^{-1}$. In the E(L104)V mutant, the P* lifetime is 5.5 ps with essentially 100% electron transfer to the L side, giving $k_{PL} \sim (5.5\ ps)^{-1}$. Taking the square root of the ratio of these rate constants yields a 2.6-fold difference in the effective electronic matrix elements favoring the L side over the M side (i.e., $V_L/V_M = 2.6$). What if $P^+BChl_M^-$ is not below P* in free energy in the YFH mutant? One can anticipate that pushing this state below P* to achieve the "matched" situation would result in a faster (or at worst unchanged) rate of electron transfer to the M side, making the ratio of electronic matrix elements even smaller than 2.6.

Other comparisons also give a modest ratio of the L/M electronic matrix elements. For example, it is highly plausible

[6] In the YFH mutant, the higher free energy of $P^+BChl_L^-$ and lower free energy of $P^+BChl_M^-$ result from a respective loss and gain of an effect of the OH dipole of Tyr on the $BChl^-$/BChl potentials. In the DH and KDH mutants, the analogous effects derive from the addition of ionizable Lys and Asp near the BChls. The free energy and redox shifts do not require Lys or Asp to be ionized and could result from the effects of dipoles of the neutral forms of the residues. Resonance Raman experiments on the G(M201)D mutant are consistent with Asp M201 being ionized, at least at room temperature (*40*). Whether Tyr M208 or Asp M201 has the larger effect on $BChl_L$ depends on many factors (ionization state, dielectric screening, and distance/orientation/position of the groups with respect to the cofactors, etc.). The results for the YFH, KDH, and DH mutants indicate that Asp M201 and Tyr M208 shift the free energy of $P^+BChl_L^-$ by comparable amounts.

[7] One can anticipate some mismatch between the free energies of $P^+BPh_L^-$ and $P^+BPh_M^-$ (and $P^+BChl_L^-$ and $P^+BChl_M^-$), as well as the reorganization energies for formation of these states, in this "near perfect" scenario. However, these mismatches should give only modest perturbations to the arguments presented here and not substantively alter the conclusions.

that both $P^+BChl_M^-$ and $P^+BChl_L^-$ are slightly above P* in the YFH and KDH mutants. In support of this idea, Stark effect spectra (*49*, *50*) and resonance Raman measurements (*51*) indicate that the L-side cofactors may experience an effective larger dielectric constant than those on the M side, and calculations indicate a related gradient of electrostatic potential across the RC (*19*). Thus, equivalent amino acid changes could well result in a smaller effect on the free energy of a charge-separated state on the M side than on the L side. It follows that $P^+BChl_L^-$ could be destabilized more than $P^+BChl_M^-$ is stabilized upon loss of Tyr M208 and gain of Tyr L181, respectively. Calculations are consistent with this possibility, although the difference is not large (*18*). If indeed both $P^+BChl_M^-$ and $P^+BChl_L^-$ are slightly above P* in the YFH mutant, then we compare $(18\ ps)^{-1}$ for L-side charge separation with $(37\ ps)^{-1}$ for M-side charge separation (Table 1).[8] This comparison yields a value of only 1.4 for the ratio V_L/V_M of the L- and M-side electronic matrix elements.

This analysis, which encompasses the cases that $P^+BChl_M^-$ is above P* or below it in the YFH mutant, yields a range of 2−7 (1.4^2 to 2.6^2) for the contribution of the electronic factor to the *overall* 30-fold (*or larger*) difference in the rates of charge separation to the L and M sides in the wild-type RC (*31*, *52*, *53*). Other things being equal (e.g., reorganization energies), these values imply that the contribution of the relative electronic matrix elements to the inherent L-side directionality of electron transfer may be as large as about 60% or at the other extreme about 10%, with balance of course derived from energetic considerations.[9] The results on the *Rb. sphaeroides* H(M182)L mutant imply similar conclusions (*44*). The finding of comparable rates of energy transfer from the two sides of the RC to P (if occurring by the Dexter exchange mechanism) also may limit the importance of the relative electronic matrix elements for unidirectional charge separation (*54*). Although there is general agreement that the effective L-side electronic matrix element is larger than that on the M side, some calculations predict a modest contribution of the asymmetry of electronic matrix elements to directionality, while others suggest this may be the preponderant effect (*20*, *55*−*61*). The idea that the relative free energies of $P^+BChl_L^-$ and $P^+BChl_M^-$ with respect to P* and the consequent effects on the associated mechanisms and rates play a substantial role in directionality was raised in early calculations (*5*). A handful of recent experimental studies, including the studies reported here, leave no doubt that the free energies of these states and the energetics in general make a substantial contribution to directionality (*23*, *24*, *31*, *44*). The results reported here provide relatively straightforward experimental findings that suggest that the contribution of electronic matrix elements is at most comparable to role of energetics, but is not overwhelmingly dominant.

The results we have presented here also have implications for the previously studied L181 and M208 mutants. Specifically, we can make the some predictions for the YF mutant in *Rb. capsulatus* via the following simplified, but useful, exercise.[10] First we set $k_{PM} = (36\ ps)^{-1}$ and $k_{PG} = (100\ ps)^{-1}$ based on the results on the YFH, DH, and KDH mutants. A reasonable estimate of $(8\ ps)^{-1}$ for the value of k_{PL} is obtained as follows. Since the $\sim(18\ ps)^{-1}$ value of k_{PL} in the YFH mutant is 2-fold larger than that of $\sim(9\ ps)^{-1}$ in the H mutant, we will set k_{PL} in the YF mutant a factor of 2 larger than the rate constant of $\sim(4\ ps)^{-1}$ in wild-type. Using these values, one calculates the following yields of the decay products of P* in the YF mutant: 6% ground-state recovery, 17% $P^+BPh_M^-$ formation, and 77% $P^+BPh_L^-$. One might be able to discern some spectral evidence in the Q_X region for $P^+BPh_M^-$ if the yield is this high, though arriving at an accurate value for the yield would be difficult. In the anion region, one should more clearly observe biexponential decay kinetics reflecting the lifetimes of $P^+BPh_L^-$ and $P^+BPh_M^-$. P bleaching should decay with biexponential kinetics also, reflecting the lifetimes of P* and $P^+BPh_M^-$, both of which involve decay to the ground state (the latter in the absence of Q_B). Finally, a P bleaching at long times (several nanoseconds) that is reduced to ~77% of its initial magnitude should be readily detected. This analysis also predicts a P* lifetime of ~6 ps. Interestingly, Jia et al. found a P* lifetime in the *Rb. capsulatus* YF mutant that, while apparently multiexponential, had an "average" value of ~9 ps (*10*). Most of the previous time-resolved studies on the *Rb. capsulatus* M208 and *Rb. sphaeroides* M210 single mutants have focused on the P* lifetimes and attendant issues regarding the mechanism (one versus two steps) of electron transfer to the L side. Some 10 years have passed since this pioneering work on the M208/M210 mutants was first reported. With the advantage of hindsight from today's perspective, it would be interesting to reinvestigate some of these mutants, and also those L181 mutants that stabilize $P^+BChl_M^-$, with an eye toward the possibility that electron transfer to the M side may occur. Also, renewed studies on the heterodimer mutants might be informative.

[8] One caveat is that the L-side electron acceptor is a BChl (β) and on the M side it is a BPh (BPh_M). However, there should be a reasonably good match in the free energies of these two states—both higher than $P^+BPh_L^-$ in wild-type and still below P*. This is aided by the fact that BChl (β) is harder to reduce than BPh and the generally higher free energies of the states on the M side.

[9] We have specifically referred here to the "effective electronic matrix elements" for L- versus M-side electron transfer to avoid ambiguity with the varied uses of electronic "couplings", "factors", "mixings", "contributions", and "matrix elements" in the literature (*20*, *55*−*62*). By electronic matrix elements, we specifically refer to the contributions of orbital overlaps and electron density distributions, and how these come into play (including addition/cancellation of wave functions) in determining the electronic interactions between the relevant electronic states. The issues can become clouded in perspective, basis set, and language if (as is most likely the case) the relative contributions of one- and two-step mechanisms differ on the two sides due predominantly to the relative (free) energies of $P^+BChl_L^-$ and $P^+BChl_M^-$ with respect to P*. This is so because in the superexchange mechanism the "electronic couplings" involve both electronic matrix elements and energy gaps (denominators). Thus, we are trying here to address the relative contributions to directionality of (1) the relative free energies of the states on the L and M branches (which necessarily includes effects on relative mechanisms) and (2) electronic matrix elements as defined above. This perspective often has been taken in considering the origins of directionality.

[10] The following discussion applies to the YF mutant specifically in *Rb. capsulatus*. A somewhat lower yield of M-side electron transfer will probably be obtained in the *Rb. sphaeroides* YF mutant. About a factor of 2 lower yield of $P^+BPh_M^-$ is found in both the DH and H *Rb. sphaeroides* mutants compared to the *Rb. capsulatus* analogues (*63*).

REFERENCES

1. Ermler, U., Fritzsch, G., Buchanan, S., and Michel, H. (1994) *Structure 2*, 925−936.

2. Deisenhofer, J., Epp, O., Sinning, I., and Michel, H. (1995) *J. Mol. Biol. 246*, 429−457.
3. Yeates, T. O., Komiya, H., Chirino, A., Rees, D. C., Allen, J. P., and Feher, G. (1988) *Proc. Natl. Acad. Sci. U.S.A. 85*, 7993−7997.
4. El-Kabbani, O., Chang, C.-H., Tiede, D., Norris, J., and Schiffer, M. (1991) *Biochemistry 30*, 5361−5369.
5. Parson, W. W., Chu, Z.-T., and Warshel, A. (1990) *Biochim. Biophys. Acta 1017*, 251−272.
6. Nagarajan, V., Parson, W. W., Gaul, D., and Schenck, C. C. (1990) *Proc. Natl. Acad. Sci. U.S.A. 87*, 7888−7892.
7. Nagarajan, V., Parson, W. W., Davis, D., and Schenck, C. C. (1993) *Biochemistry 32*, 12324−12336.
8. Chan, C.-K., Chen, L. X.-Q., DiMagno, T. J., Hanson, D. K., Nance, S. L., Schiffer, M., Norris, J. R., and Fleming, G. R. (1991) *Chem. Phys. Lett. 176*, 366−372.
9. Du, M., Rosenthal, S. J., Xie, X., DiMagno, T. J., Schmidt, M., Hanson, D. K., Schiffer, M., Norris, J. R., and Fleming, G. R. (1992) *Proc. Natl. Acad. Sci. U.S.A. 89*, 8517−8521.
10. Jia, Y., DiMagno, T. M., Chan, C.-K., Wang, Z., Du, M., Hanson, D. K., Schiffer, M., Norris, J. R., Fleming, G. R., and Popov, M. S. (1993) *J. Phys. Chem. 97*, 13180−13191.
11. Finkele, C., Lauterwasser, W., Zinth, K. A., Gray, and Oesterhelt, D. (1990) *Biochemistry 29*, 8517−8521.
12. Hamm, P., Gray, K. A., Oesterhelt, D., Feick, R., Scheer, H., and Zinth, W. (1993) *Biochim. Biophys. Acta 1142*, 99−105.
13. Beekman, L. M. P., van Stokkum, I. H. M., Monshouwer, R., Rijnders, A. J., McGlynn, P., Visschers, R. W., Jones, M. R., and van Grondelle, R. (1996) *J. Phys. Chem. 100*, 7256−7268.
14. Laible, P. D., Greenfield, S. R., Wasielewski, M. R., Hanson, D. K., and Pearlstein, R. M. (1997) *Biochemistry 36*, 8677−8685.
15. Gray, K. A., Wachtveitl, J., and Oesterhelt, D. (1992) *Eur. J. Biochem. 207*, 723−731.
16. Streltsov, A. M., Vulto, S. I. E., Shkuropatov, A. Ya., Hoff, A. J., Aartsma, T. J., and Shuvalov, V. A. (1998) *J. Phys. Chem. B 102*, 7293−7298.
17. Zhou, H., and Boxer, S. G. (1998) *J. Phys. Chem. B 102*, 9139−9147.
18. Alden, R. G., Parson, W. W., Chu, Z. T., and Warshel, A. (1996) *J. Phys. Chem. 100*, 16761−16770.
19. Gunner, M. R., Nicholls, A., and Honig, B. (1996) *J. Phys. Chem. 100*, 4277−4291.
20. Bixon, M., Jortner, J., and Michel-Beyerle, M. E. (1995) *Chem. Phys. 197*, 389−404.
21. Volk, M., Aumeier, G., Langenbacher, T., Feick, R., Ogrodnik, A., and Michel-Beyerle, M. E. (1998) *J. Phys. Chem. B 102*, 735−751.
22. Schmidt, S., Arlt, T., Hamm, P., Huber, H., Nagele, T., Wachtveitl, J., Meyer, M., Scheer, H., and Zinth, W. (1994) *Chem. Phys. Lett. 223*, 116−120.
23. Kirmaier, C., Weems, D., and Holten, D. (1999) *Biochemistry 38*, 11516−11530.
24. Roberts, J. A., Holten, D., and Kirmaier, C. (2001) *J. Phys. Chem. B 105*, 5575−5584.
25. Gunner, M. (1991) *Curr. Top. Bioenerg. 16*, 319.
26. Goldstein, R. A., and Boxer, S. G. (1989) *Biochim. Biophys. Acta 977*, 70−77.
27. Peloquin, J. M., Williams, J. C., Lin, X., Alden, R. G., Taguchi, A. K. W., Allen, J. P., and Woodbury, N. W. (1994) *Biochemistry 33*, 8089−8100.
28. Hartwich, G., Lossau, H., Michel-Beyerle, M. E., and Ogrodnik, A. (1998) *J. Phys. Chem. B 102*, 3815−3820.
29. Woodbury, N. W., Becker, M., Middendorf, D., and Parson, W. W. (1985) *Biochemistry 24*, 7516−7521.
30. Fleming, G. R., Martin, J.-L., and Breton, J. (1988) *Nature* (*London*) *33*, 190−192.
31. Heller, B. A., Holten, D., and Kirmaier, C. (1995) *Science 269*, 940−945.
32. Williams, J. C., Alden, R. H., Murchison, H. A., Peloquin, J. M., Woodbury, N. W., and Allen, J. P. (1992) *Biochemistry 31*, 11029−11037.
33. Kirmaier, C., Gaul, D., DeBey, R., Holten, D., and Schenck, C. C. (1991) *Science 251*, 922−927.
34. Kirmaier, C., Laporte, L., Schenck, C. C., and Holten, D. (1995) *J. Phys. Chem. 99*, 8910−8917.
35. Heller, B. A., Holten, D., and Kirmaier, C. (1996) *Biochemistry 35*, 15418−15427.
36. Bylina, E. J., and Youvan, D. C. (1988) *Proc. Natl. Acad. Sci. U.S.A. 85*, 7226−7230.
37. Laible, P. D., and Hanson, D. K., manuscript in preparation.
38. Kirmaier, C., and Holten, D. (1991) *Biochemistry 30*, 609−613.
39. Yang, S. I., Li, J., Cho, H. S., Kim, D., Bocian, D. F., Holten, D., and Lindsey, J. S. (2000) *J. Mater. Chem. 10*, 283−296.
40. Czarnecki, K., Kirmaier, C., Holten, D., and Bocian, D. F.-(1999) *J. Phys. Chem. A 103*, 2235−2246.
41. Thompson, M. A., Zerner, M. C., and Fajer, J. (1991) *J. Am. Chem. Soc. 113*, 8210−8215.
42. Marchi, M., Gehlen, J. N., Chandler, D., and Newton, M. (1994) *Science 263*, 499−502.
43. Blomberg, M. R. A., Siegbahn, P. E. M., and Babcock, G. T. (1998) *J. Am. Chem. Soc. 120*, 8812−8824.
44. Katilius, E., Turanchik, T., Lin, S., Taguchi, A. K. W., and Woodbury, N. W. (1989) *J. Phys. Chem. B 103*, 7386−7389.
45. Fajer, J., Borg, D. C., Forman, A., Dolphin, D., and Felton, R. H. (1973) *J. Am. Chem. Soc. 95*, 2739−2741.
46. Fajer, J., Brune, D. C., Davis, M. S., Forman, A., and Spaulding, L. D. (1975) *Proc. Natl. Acad. Sci. U.S.A. 72*, 4956−4960.
47. Cotton, T. M., and Van Duyne, R. P. (1979) *J. Am. Chem. Soc. 101*, 7605−7612.
48. Felton, R. (1978) in *The Porphyrins* (Dolphin, D., Ed.) Vol V, pp 53−125, Academic Press, New York.
49. Steffen, M. A., Lao, K., and Boxer S. G. (1994) *Science 264*, 810−816.
50. van Dijk, B., Hoff, A. J., and Shkuropatov, A. Ya. (1998) *J. Phys. Chem. B 102*, 8091−8099.
51. Palaniappan, V., and Bocian, D. F. (1995) *J. Am. Chem. Soc. 117*, 3447−3448.
52. Bixon, M., Jortner, J., Michel-Beyerle, M. E., and Ogrodnik, A. (1989) *Biochim. Biophys. Acta 977*, 273−286.
53. Kellogg, E. C., Kolaczkowski, S., Wasielewski, M. R., and Tiede, D. M. (1989) *Photosynth. Res. 22*, 47−59.
54. King, B. A., deWinter, A., McAnaney, T. B., and Boxer, S. G. (2001) *J. Phys. Chem. B 105*, 1856−1862.
55. Scherer, P. O. J., and Fischer, S. F. (1989) *Chem. Phys. 131*, 115−127.
56. Zhang, L. Y., and Friesner, R. A. (1998) *Proc. Natl. Acad. Sci. U.S.A. 95*, 13603−13605.
57. Michel-Beyerle, M. E., Plato, M., Deisenhofer, J., Michel, H., Bixon, M., and Jortner, J. (1988) *Biochim. Biophys. Acta 932*, 52−70.
58. Plato, M., Mobius, K., Michel-Beyerle, M. E., Bixon, M., and Jornter, J. (1988) *J. Am. Chem. Soc. 110*, 7279−7285.
59. Ivashin, N., Kallenbring, B., Larsson, S., and Hansson, O. (1998) *J. Phys. Chem. B 102*, 5017−5022.
60. Hasegawa, J., and Nakatsuji, H. (1998) *J. Phys. Chem. B 102*, 10420−10439.
61. Kolbasov, D., and Scherz, A. (2000) *J. Phys. Chem. B 104*, 1802−1809.
62. Warshel, A., Creighton, S., and Parson, W. W. (1988) *J. Phys. Chem. 92*, 2694−2701.
63. Kirmaier, C., Czarnecki, K., Laible, P. D., Hanson, D. K., Bocian, D. F., and Holten, D., manuscript in preparation.

BI0113263